

Mussel-Inspired Polymer Carpets: Direct Photografting of Polymer Brushes on Polydopamine Nanosheets for Controlled Cell Adhesion

Daniel Hafner, Lisa Ziegler, Muhammad Ichwan, Tao Zhang, Maximilian Schneider, Michael Schiffmann, Claudia Thomas, Karsten Hinrichs, Rainer Jordan,* and Ihsan Amin*

Polydopamine (PDA), a mussel-inspired protein, has received great attention since the seminal work of Messersmith and co-workers was published.^[1] Undoubtedly, that work has paved the way for a new strategy for surface modification and functionalization via simple chemistry.^[2] Due to its excellent adhesive properties, PDA can be grafted on various substrates; this has triggered further exploitation for its utilization in a wide range of applications in surface coatings,^[3,4] in biotechnology and medicine,^[5,6] in water purification membranes,^[7] sensors,^[8] and energy such as for organic conductive electrode and solar cells.^[9]

It is well known that PDA is robust and has good mechanical stability^[10,11] owing to its nature of self-crosslinking. Using this knowledge, we report in this communication on the preparation of 2D PDA nanosheets, with thicknesses of tens of nanometers and lateral sizes up to centimeters, as functional surface for grafting various polymer brushes, leading to freestanding mussel-inspired polymer carpets. The polymer brushes can be simply grafted on PDA nanosheet via self-initiated photografting and photopolymerization (SIPGP), while no catalyst is needed. We demonstrate that the PDA nanosheets

and their polymer brushes derivatives show lateral integrity, that these sheets are robust and therefore can be detached from their substrates. The freestanding films are stable under harsh condition, such as a hydrogen fluoride (HF) solution, during and after film detachment. Cell adhesion tests show that PDA nanosheets promote cell growth and attachment, while a PDA-based poly(3-sulfopropyl methacrylate) carpet exhibits non-fouling properties. We expect that PDA nanosheets as a new platform of functional 2D material and their polymer carpet derivatives will find numerous applications in surface coatings, biotechnology, and medicine.

Figure 1a shows a schematic illustration of the preparation of a PDA nanosheet and its freestanding mussel-inspired polymer carpets. First, PDA was deposited on silicon (Si) substrates using a method described previously.^[1,12] For our purpose, a 12 nm thick as-grafted PDA layer was used. By etching the Si substrate with HF, the PDA layer can be detached from its substrate and a 2D PDA nanosheet can be formed and transferred to any other substrates. There are several reports on grafting polymer brushes on PDA-functionalized substrates,^[13] however none have reported the utilization of PDA nanosheets as a functional surface for directly grafting polymer brushes.

Recently, many authors have reported the utilization of the SIPGP method for directly grafting polymer brushes on surfaces without using a catalyst during the polymerization itself.^[14] It has been demonstrated that by SIPGP, highly robust and well-defined polymer brushes can be directly grafted on various surfaces.^[15,16] Frechet and co-workers showed that the initiator-free SIPGP method relies on a radical abstraction mechanism during UV irradiation and uses the monomer itself as photosensitizer.^[17] As the PDA nanosheet bears amino and hydroxyl functional groups, the hydrogen from the amino and hydroxyl groups can be abstracted upon UV irradiation, generating radicals that later initiate the polymerization. Thus, SIPGP is also a suitable method for grafting polymer brushes on 2D PDA nanosheets, leading to the fabrication of freestanding mussel-inspired polymer carpets. In Figure 1b, an as-grafted PDA layer on SiO₂ and PDA nanosheets before and after SIPGP with poly(styrene) (PS) and poly(*N,N*-dimethylamino)ethyl methacrylate (PDMAEMA) are shown. The color differences reveal not only different thicknesses but also different polymer grafts. A swollen 60 nm thick PDA nanosheet was obtained from detachment of a 12 nm thick as-grafted PDA layer. In Figure 1b, the polymer carpets of PDA nanosheets after SIPGP with styrene for 18 h and PDMAEMA for 2 h are shown. For our study, we have grafted not only PS and PDMAEMA,

D. Hafner, L. Ziegler, T. Zhang,
M. Schneider, M. Schiffmann, Dr. C. Thomas,
Prof. R. Jordan, Dr. I. Amin
Makromolekulare Chemie
Technische Universität Dresden
Mommsenstrasse 4, 01069 Dresden, Germany
E-mail: rainer.jordan@tu-dresden.de;
ihsan.amin@chemie.tu-dresden.de



M. Ichwan
Center for Regenerative Therapy Dresden
Fetscherstrasse 105, 01307 Dresden, Germany
M. Ichwan
Department of Pharmacology and Therapeutic
Faculty of Medicine
Universitas Sumatera Utara
Jalan Dr. T. Mansur 5, 20155 Medan, Indonesia
Dr. K. Hinrichs
Leibniz-Institut für Analytische
Wissenschaften-ISAS-e.V., Department Berlin
Schwarzschildstrasse 8, 12489 Berlin, Germany
Prof. R. Jordan, Dr. I. Amin
Center for Advancing Electronics Dresden
Technische Universität Dresden
George-Schumannstrasse 11, 01187 Dresden, Germany

DOI: 10.1002/adma.201504033

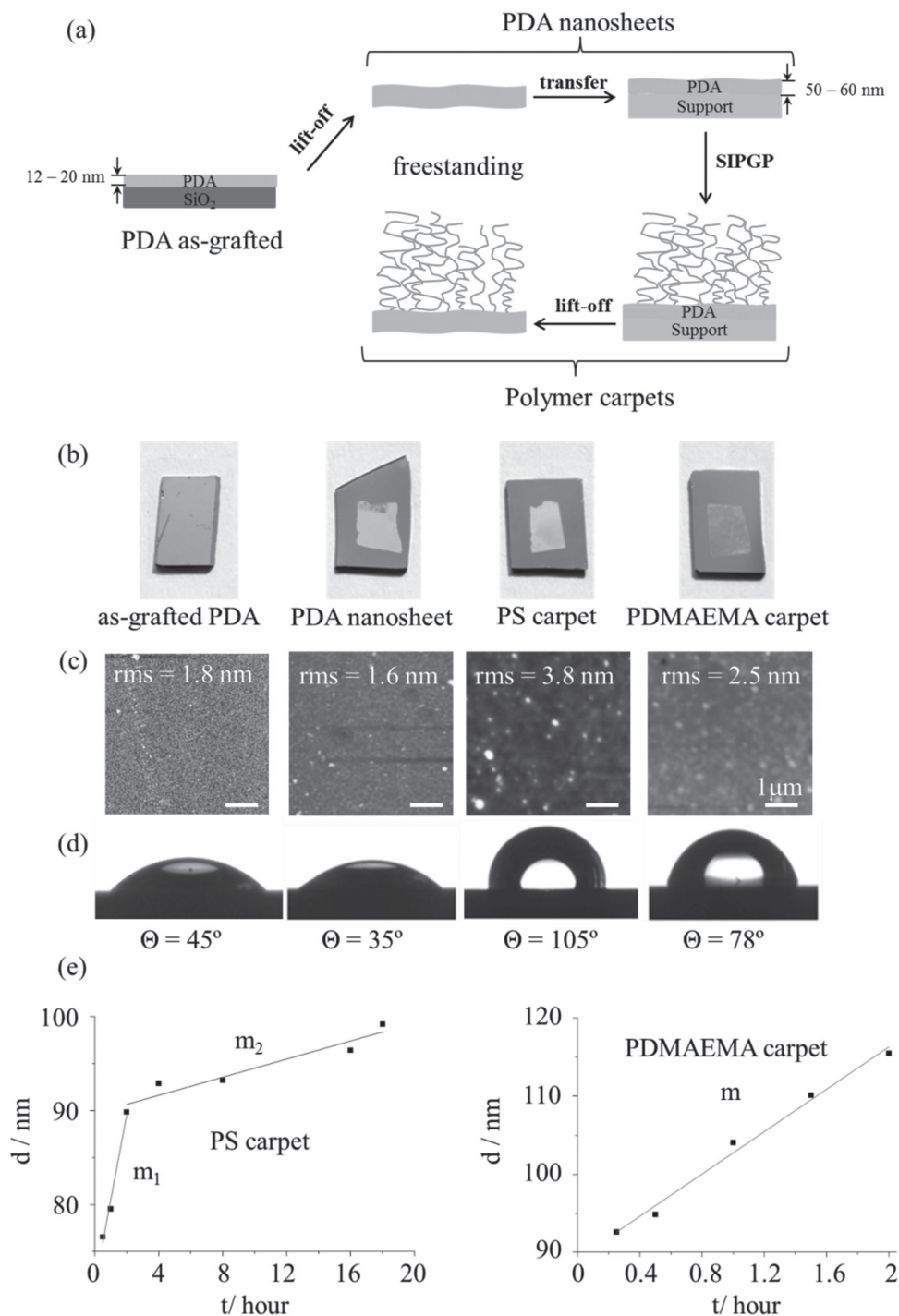


Figure 1. a) Schematic illustration of preparation of a PDA nanosheet and its freestanding polymer carpets. b) As-grafted PDA layer and PDA nanosheet before and after SIPGP with poly(styrene) (PS) for 18 h and PDMAEMA for 2 h. c) AFM height scan image of (b). d) Water contact angle of (b). e) Thickness evolution of polymer brushes grafted on PDA nanosheets as function of polymerization time for a PS carpet and a PDMAEMA carpet.

but also poly(methylmethacrylate) (PMMA), poly(4-vinylpyridine) (P4VP), poly(3-sulfopropyl methacrylate) (PSPMA), and poly(*tert*-butyl acrylate) (P*t*BuA) (Figure S1, Supporting Information). Ellipsometry measurements reveal that the thicknesses of PDA-based polymer carpets are 108 nm for PS, 80 nm for PDMAEMA, 127 nm for PMMA, 94 nm for P4VP, 83 nm

for PSPMA, and 88 nm for P*t*BuA (Table S1, Supporting Information). The simplicity of preparing diverse polymer brushes on PDA nanosheets demonstrates the easiness and novelty of SIPGP for polymerization. Furthermore, atomic force microscopy (AFM) was performed to determine the surface roughness of the samples (Figure 1c); water static contact angle

(CA) measurements (Figure 1d) were performed on PDA nanosheets, before and after polymerization to obtain information on the wettability of the samples. As shown in Figure 1c, an as-grafted PDA layer has a root-mean-square (rms) surface roughness of 1.8 nm as revealed by AFM with contact angle of 45°, which is in good agreement with the literature.^[1,4,18] Interestingly, after detachment, a PDA nanosheet becomes more hydrophilic with a contact angle = 35°, lower than that of an as-grafted PDA layer. This may be attributed to the hygroscopic nature of PDA. The morphology of PDA nanosheet, as revealed by AFM, is smooth with a surface roughness of 1.6 nm. After polymerization with styrene for 18 h, the surface becomes hydrophobic with a contact angle = 105°. This value is higher than reported in literature.^[19] However, this can be explained by the rougher morphology as revealed by AFM: a surface roughness of 3.8 nm was found for the PS carpet. For PDMAEMA, the surface roughness is 2.5 nm, lower than that of a PS carpet. A contact angle of 78° was found, which is in agreement with the literature.^[20] For PMMA, P4VP, PSPMA, and P*t*BuA carpets, the water contact angles are 62°, 54°, 12°, and 90°, respectively (Table S2, Supporting Information). The change in wettability before and after SIPGP indicates the successful grafting of the polymer brushes on PDA nanosheets. Furthermore, infrared spectroscopic ellipsometry^[21] was performed as an additional confirmation to prove the success of grafting of polymer brushes on PDA nanosheets, as discussed in the Supporting Information.

Next, for both PS and PDMAEMA, height dependency on polymerization time was investigated. Interestingly, we observed different grafting behavior for PS and PDMAEMA carpets. As shown in Figure 1e, for PS, at the beginning of polymerization time (shorter than 3 h) a steep increase in polymer brush thickness and higher growth rate were observed ($m_1 = 9.06 \text{ nm h}^{-1}$). However, after 3 h, polymerization slows down and the growth rate is more than 20-fold lower ($m_2 = 0.48 \text{ nm h}^{-1}$). We assume that this different grafting behavior is due to a strong mismatch or similar wettability between the monomer used and PDA. PDA is very hydrophilic and when a water-insoluble hydrophobic monomer such as styrene is used, it is plausible that a strong hydrophobic–hydrophilic mismatch interaction will occur during polymerization. As SIPGP utilizes UV light for photopolymerization, the longer the polymerization, the more homopolymer, in this case, PS, is created in solution. As PS is hydrophobic and water-insoluble, it creates a bad solvent condition and PDA collapses. Once the homopolymer dominates the system, a kinetic barrier will be formed and polymerization slows down. The condition is different when a water-soluble hydrophilic monomer such as DMAEMA is used. For PDMAEMA, a linear relationship between thickness and polymerization time with a high growth rate 13.54 nm h⁻¹ is observed. Due to similar wettability of PDA and DMAEMA, the

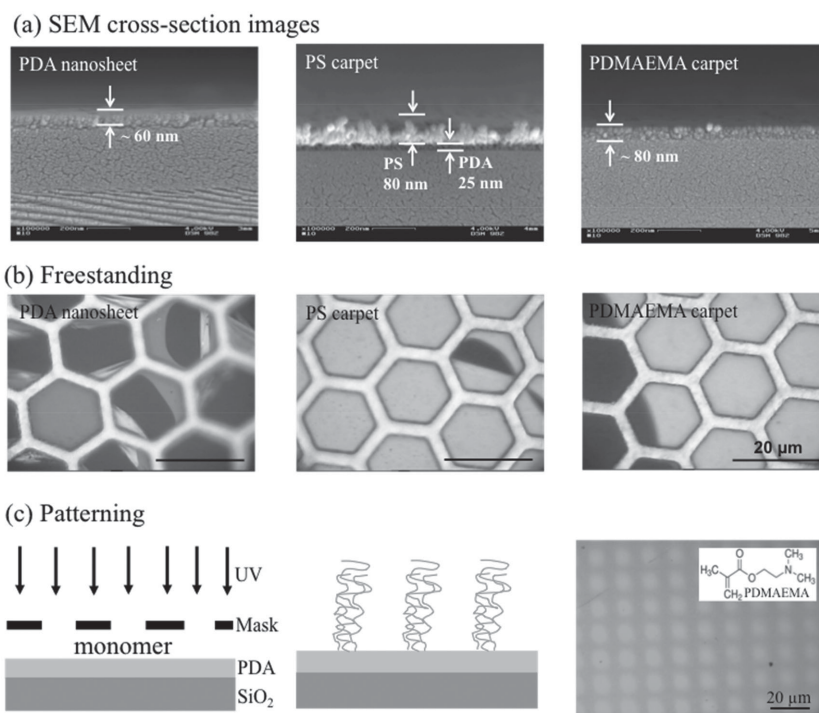


Figure 2. a) SEM cross-section image of PDA nanosheet, PS carpet and PDMAEMA carpet. b) Optical images of freestanding PDA (left), freestanding PS carpet (middle), and freestanding PDMAEMA carpet (right) suspended on TEM grid. c) Schematic illustration of fabrication of patterned PDMAEMA carpet on PDA nanosheet.

molecules of DMAEMA monomer can probably diffuse into the PDA layer and the polymerization starts not only on the surface, but also within the layer. This leads to a linear relationship between polymerization time and brush thickness.

Scanning electron microscopy (SEM) cross-section images are presented in Figure 2a. From the cross-section, the thickness of PDA carpet is calculated to be about 54 nm, which corroborates the data from the IR spectroscopic ellipsometry (56 nm). Interestingly, for a PS carpet, the cross-section SEM image reveals a two-layer composition with a total thickness of 105 nm, which is similar to the thickness obtained from IR ellipsometry (108 nm). The observation of two distinct layers on PDA-based PS carpet supports our assumption that a mismatch in wettability occurs during deposition of a water-insoluble hydrophobic monomer such as styrene on a hygroscopic–hydrophilic surface such as a PDA nanosheet, leading to the formation of a two-layer composition. The cross-section SEM image of a PS carpet clearly distinguishes the lower PDA nanosheet from the upper PS layer. The thickness of PDA nanosheet is about 25 nm, supporting our assumption that PDA collapses (from 60 to 25 nm) during SIPGP of styrene, as styrene or polystyrene are bad solvents for PDA.

As shown in Figure 2a for PS carpet, PS layer really mimics macro-brushes, with a thickness of about 80 nm. As the upper PS layer is hydrophobic and the lower PDA nanosheet is hydrophilic, our PDA-based PS carpet can be considered as Janus polymeric membrane. For a PDMAEMA carpet, as revealed by the SEM cross-section image, the total thickness is about 80 nm. However, unlike in the PS carpet, the PDMAEMA brush

layer is indistinguishable from the PDA nanosheet. A one-layer composition has been observed, forming a PDA-PDMAEMA carpet composite. This, again, supports our assumption that, due to a similar wettability of a DMAEMA monomer and a PDA nanosheet, the monomers can diffuse within the PDA layer during SIPGP and start the polymerization not only on the surface but also within the layer, leading to indistinguishable one-layer composition. This finding on PDA nanosheet and PDA-based polymer carpets might help to fabricate Janus polymer carpets, an alternative route from a recently published one on Janus polymeric membranes.^[22]

As both PDA nanosheet and the polymer carpets are robust, the entire nanosheet and the carpets can be easily re-detached from their substrates by etching the SiO₂ substrate with HF^[15,23] and suspended on a transmission electron microscopy (TEM) grid, as shown in Figure 2b. We observed no defects on a PDA nanosheet and its polymer carpet derivatives after contact with HF. The strong color contrasts are observed for the freestanding carpets due to light diffraction, revealing different thicknesses. The freestanding nanosheet and the polymer carpets exhibit lateral integrity and relatively smooth surfaces. The processes of preparation of freestanding carpets demonstrated that both PDA nanosheet and polymer carpets are robust and stable against a harsh environment such as an HF solution. Furthermore, mechanical properties measurements on the films were performed by AFM indentation. The Young's modulus, E , of the films as determined by AFM for as-grafted PDA was 4.2 ± 0.2 GPa. This value is in agreement with that obtained by Buehler and co-workers,^[11] who reported a value of 4.1–4.4 GPa for grafted PDA layer. For transferred PDA nanosheet, a slight decrease of $E = 3.9 \pm 0.2$ GPa was found. The slight lower E value for PDA nanosheet may explain the reason we obtained lower surface roughness and contact angle for transferred PDA nanosheet as compared to PDA as-grafted. Interestingly, we have lower E after grafted with PS ($E = 2.5 \pm 0.3$ GPa) and higher E after grafting with PDMAEMA ($E = 5.8 \pm 0.5$ GPa) as compared to that for PDA nanosheet and as-grafted PDA. These findings correlate to the model of polymerization that we proposed. As seen in the cross-section SEM images in Figure 2, the polymerization with hydrophobic PS results in a two-layer system, consisting of the PDA nanosheet and the grafted PS brushes. When using the hydrophilic DMAEMA monomer, a swelling of the PDA nanosheet occurs and during UV photopolymerization, the entrapped DMAEMA monomers polymerize within the PDA layer, leading to an interpenetrated network. The indenting tip probes a composite structure with enhanced E for PDMAEMA, whereas for the PS, the indentation occurs on a brush system, which results in lower E . The latter is confirmed by which the E value is in agreement with our previous result with PS brushes grown on rigid crosslinked nanosheets.^[15]

Patterned polymer carpets on PDA nanosheets can be achieved by direct photopatterning, by placing a mask on the top of PDA nanosheet during photografting.^[24] DMAEMA is used to realize the patterned polymer carpet, while a TEM grid with hexagonal openings of 8 μm was used as a mask. This one-step patterning is schematically illustrated in Figure 2c. As shown by the optical images in Figure 2c, polymer brushes only grafted on the areas where the PDA nanosheet was exposed to

UV light, as a different contrast is observed between the area with and without polymer. This demonstrates not only the simplicity of the direct patterning but also proves selectivity during photopolymerization.

Next, the PDA nanosheet and its polymer carpet derivatives were used for cell adhesion studies. Cell adhesion plays an important role in determining the success or failure of implantation. Anchorage-dependent cells such as fibroblasts and osteoblasts need to adhere to survive.^[25] Fibroblast cells have negative charge^[26] and play a role in the production of various essential components of connective tissues such as glucoaminoglycans and collagen in fibrous tissue.^[27] As a model system in our study, mouse embryonic fibroblasts (MEFs) were used and prepared as previously described.^[28] MEFs easily grow and stick to common substrates such as glass. Compared to other primary explant cultures, MEFs are easy to establish and to maintain, proliferate rapidly to produce large numbers of cells from a single embryo within several days following explanation. For our purpose, PDA nanosheets and PSPMA carpets were transferred on transparent microslide glass substrates and used for adhesion cells test. As-grafted PDA layer grown directly on microslide glass was used as control. For each sample, cell density was calculated from three different areas and average values were calculated. Representative images for each sample are presented in Figure 3.

As shown in Figure 3a, cells have grown and spread over the as-grafted PDA layer. Interestingly, as observed in Figure 3b, about 44% more cells have grown, attached and spread on a PDA nanosheet as compared to as-grafted PDA layer. This indicates that PDA nanosheet is promoting more cells growth and attachment. The better cells growth on PDA nanosheet can be explained by the lower Young's modulus, thus softer surface, for PDA nanosheet as cells prefer to grow and attach on softer surfaces.^[29] Furthermore, after grafting negatively charged polymer brush such as PSPMA on a PDA nanosheet, the carpet inhibits cell growth and attachment, consequently, significantly 75% fewer cells grown on PSPMA carpet. Moreover, it is also worth noticing that, while most of the cells observed on PDA nanosheet have a spreading shape, on a PSPMA carpet the cells have a round shape, demonstrating that on a PSPMA carpet not only fewer cells have grown but also that the attached cells are mostly repelled from the surface, forming the round shape which indicates the cells are dead, which can be easily washed away. This shows the effectiveness of PSPMA carpets as a non-fouling surface.

To summarize, we have reported the exploitation of PDA nanosheets as a functional 2D nanosheet for directly grafting polymer carpets. We have shown that, via SIPGP, diverse polymer carpets can be prepared. SIPGP offers simplicity, since no initiator is needed and tedious multistep polymerizations such as surface-initiated pretreatment can be avoided. When hydrophobic polymer brushes are grafted on a hydrophilic PDA nanosheet, a distinct two-layer Janus-like membranes is formed while indistinguishable layer with enhanced Young's modulus is formed when a hydrophilic polymer brush is grafted on hydrophilic PDA nanosheet. Furthermore, we demonstrated that the PDA nanosheet and its freestanding polymer carpet derivatives show lateral integrity; they are robust and stable against harsh conditions such as an HF solution and the transfer process

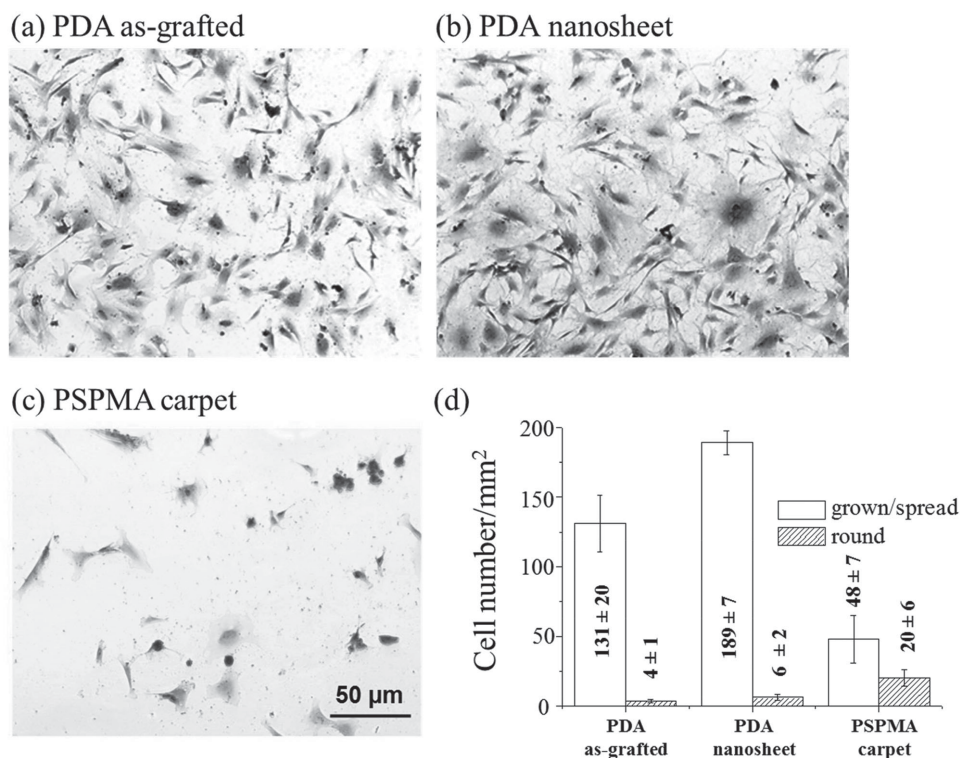


Figure 3. Representative photomicroscopy images of MEFs on a) as grafted-PDA (control sample), b) PDA nanosheet, and c) PDA-based PSPMA carpet transferred on a glass substrate, respectively. d) Comparison of the MEFs cells density on the surfaces of the samples.

itself. Patterned carpets can be realized by direct photografting when a photomask is placed on the top of the PDA nanosheet. Cell adhesion tests show that a PDA nanosheet promotes cell growth and attachment, while a PDA-based PSPMA carpet exhibits nonfouling properties. We hope these results add a new method for utilization of the PDA nanosheets and their polymer carpet derivatives and may find their application in surface coatings, biotechnology, and medicine.

Supporting Information

Supporting Information is available from the Wiley Online Library or from the author.

Acknowledgements

D.H. and L.Z. contributed equally to this work. I.A. and R.J. thank the cluster of excellence, Center for Advancing Electronics Dresden (CfAED), for financial support. M.I. thanks the DAAD for a fellowship. Support from Prof. G. Kempermann is acknowledged. T.Z. thanks the China Scholarship Council (CSC) from P. R. China for a Ph.D. grant. C.T. acknowledges the funding from ESF-Nachwuchsforschergruppe ChemIT—“Chemische Informationstechnik”. K.H. thanks I. Fischer for her valuable technical assistance, as well as financial support from the Senatsverwaltung für Wirtschaft, Technologie und Forschung des Landes Berlin und Bundesministerium für Bildung und Forschung.

Received: August 18, 2015

Revised: October 15, 2015

Published online: December 15, 2015

- [1] H. Lee, S. M. Dellatore, W. M. Miller, P. B. Messersmith, *Science* **2007**, *318*, 426.
- [2] D. R. Dreyer, D. J. Miller, B. D. Freeman, D. R. Paul, C. W. Bielawski, *Chem. Sci.* **2013**, *4*, 3796.
- [3] a) V. Ball, D. Frari, M. Michel, M. Buehler, V. R. Toniazzi, M. Singh, J. Gracio, D. Ruch, *BioNanoSci.* **2012**, *2*, 16; b) Q. Ye, F. Zhou, W. M. Liu, *Chem. Soc. Rev.* **2011**, *40*, 4244; c) H. Lee, B. P. Lee, P. B. Messersmith, *Nature* **2007**, *448*, 338; d) L. Q. Guo, Q. Liu, G. L. Li, J. B. Shi, J. Y. Liu, T. Wang, G. B. Jiang, *Nanoscale* **2012**, *4*, 5864; e) W. Wei, J. Yu, C. Broomell, J. N. Israelachvili, J. H. Waite, *J. Am. Chem. Soc.* **2013**, *135*, 377; f) S. M. Kang, I. You, W. K. Cho, H. K. Shon, T. G. Lee, I. S. Choi, J. M. Karp, H. Lee, *Angew. Chem. Int. Ed.* **2010**, *49*, 9401; g) V. Ball, *Biointerphases* **2014**, *9*, 030801; h) H. Shen, J. Guo, H. Wang, N. Zhao, J. Xu, *ACS App. Mater. Interfaces* **2015**, *7*, 5701; i) H. Hu, B. Yu, Q. Ye, Y. Gu, F. Zhou, *Carbon* **2010**, *48*, 2347.
- [4] J. H. Jiang, L. P. Zhu, L. J. Zhu, B. K. Zhu, Y. Y. Xu, *Langmuir* **2011**, *27*, 14180.
- [5] a) M. B. Kai, S. Pawel, *Biofabrication* **2013**, *5*, 045009; b) H. W. Chien, W. H. Kuo, M. J. Wang, S. W. Tsai, W. B. Tsai, *Langmuir* **2012**, *28*, 5775; c) H. W. Chien, W. B. Tsai, *Acta Biomater.* **2012**, *8*, 3678; d) S. H. Ku, J. S. Lee, C. B. Park, *Langmuir* **2010**, *26*, 15104; e) K. Sun, Y. Y. Xie, D. K. Ye, Y. Y. Zhao, Y. Cui, F. Long, W. Zhang, X. Y. Jiang, *Langmuir* **2012**, *28*, 2131; f) X. Liu, J. Cao, H. Li, J. Li, Q. Jin, K. Ren, J. Ji, *ACS Nano* **2013**, *7*, 9384; g) Y. Dang, C.-M. Xing, M. Quan, Y.-B. Wang, S.-P. Zhang, S. Shi, Y. Gong, *J. Mater. Chem. B* **2015**, *10*, 4181.
- [6] a) M. E. Lyngge, P. Schattling, B. Städler, *Nanomedicine (London, U.K.)* **2015**, *10*, 2725; b) C. Rodriguez-Emmenegger, C. M. Preuss, B. Yameen, O. Pop-Georgievski, M. Bachmann, J. O. Mueller, M. Bruns, A. S. Goldmann, M. Bastmeyer, C. Barner-Kowollik, *Adv. Mater.* **2013**, *25*, 6123; c) M. E. Lyngge, R. van der Westen, A. Postma, B. Städler, *Nanoscale* **2011**, *3*, 4916.

- [7] a) C. Cheng, S. Li, J. Zhao, X. X. Li, Z. Y. Liu, L. Ma, X. Zhang, S. D. Sun, C. S. Zhao, *Chem. Eng. J.* **2013**, *228*, 468; b) M. Guvendiren, D. A. Brass, P. B. Messersmith, K. R. Shull, *J. Adhesion* **2009**, *85*, 631.
- [8] S.-H. Hwang, D. Kang, R. S. Ruoff, H. S. Shin, Y.-B. Park, *ACS Nano* **2014**, *8*, 6739.
- [9] a) H. J. Nam, B. Kim, M. J. Ko, M. Jin, J. M. Kim, D. Y. Jung, *Chem. Eur. J.* **2012**, *18*, 14000; b) Y. F. Wei, J. H. Kong, L. P. Yang, L. Ke, H. R. Tan, H. Liu, Y. Z. Huang, X. W. Sun, X. H. Lu, H. J. Du, *J. Mater. Chem. A* **2013**, *1*, 5045; c) R. Li, K. Parvez, F. Hinkel, X. Feng, K. Müllen, *Angew. Chem. Int. Ed.* **2013**, *52*, 5535.
- [10] a) N. F. Della Vecchia, R. Marega, M. Ambrico, M. Iacomino, R. Micillo, A. Napolitano, D. Bonifazi, M. d'Ischia, *J. Mater. Chem. C* **2015**, *3*, 6525; b) M. d'Ischia, A. Napolitano, V. Ball, C. T. Chen, M. J. Buehler, *Acc. Chem. Res.* **2014**, *47*, 3541.
- [11] S. C. Lin, C. T. Chen, I. Bdkin, V. Ball, J. Gracio, M. J. Buehler, *Soft Matter* **2014**, *10*, 457.
- [12] a) S. M. Kang, N. S. Hwang, J. Yeom, S. Y. Park, P. B. Messersmith, I. S. Choi, R. Langer, D. G. Anderson, H. Lee, *Adv. Funct. Mater.* **2012**, *22*, 2949; b) V. Ball, D. Del Frari, V. Toniazzo, D. Ruch, *J. Colloid Interface Sci.* **2012**, *386*, 366.
- [13] a) Z. Ma, X. Jia, J. Hu, Z. Liu, H. Wang, F. Zhou, *J. Agric. Food Chem.* **2013**, *61*, 12232; b) M. Kohri, H. Kohma, Y. Shinoda, M. Yamauchi, S. Yagai, T. Kojima, T. Taniguchi, K. Kishikawa, *Polym. Chem.* **2013**, *4*, 2696; c) L.-N. Xiang, L.-J. Chen, L. Tan, C. Zhang, F.-H. Cao, S.-T. Liu, Y.-M. Wang, *Chin. Chem. Lett.* **2013**, *24*, 597; d) Q. Wei, B. Yu, X. Wang, F. Zhou, *Macromol. Rapid Commun.* **2014**, *35*, 1046; e) W. Sheng, B. Li, X. Wang, B. Dai, B. Yu, X. Jia, F. Zhou, *Chem. Sci.* **2015**, *6*, 2068; f) J. Tian, D. Xu, M. Liu, F. Deng, Q. Wan, Z. Li, K. Wang, X. He, X. Zhang, Y. Wei, *J. Polym. Sci., Part A: Polym. Chem.* **2015**, *53*, 1872.
- [14] a) J. P. Deng, W. T. Yang, B. Ranby, *Macromol. Rapid Commun.* **2001**, *22*, 535; b) M. Steenackers, A. Kuller, S. Stoycheva, M. Grunze, R. Jordan, *Langmuir* **2009**, *25*, 2225; c) A. N. Wright, *Nature* **1967**, *215*, 953.
- [15] a) I. Amin, M. Steenackers, N. Zhang, A. Beyer, X. H. Zhang, T. Pirzer, T. Hugel, R. Jordan, A. Golzhauser, *Small* **2010**, *6*, 1623; b) I. Amin, M. Steenackers, N. Zhang, R. Schubel, A. Beyer, A. Golzhauser, R. Jordan, *Small* **2011**, *7*, 683.
- [16] a) S. Gupta, M. Agrawal, M. Conrad, N. A. Hutter, P. Olk, F. Simon, L. M. Eng, M. Stamm, R. Jordan, *Adv. Funct. Mater.* **2010**, *20*, 1756; b) M. Steenackers, A. M. Giggler, N. Zhang, F. Deubel, M. Seifert, L. H. Hess, C. H. Y. X. Lim, K. P. Loh, J. A. Garrido, R. Jordan, M. Stutzmann, I. D. Sharp, *J. Am. Chem. Soc.* **2011**, *133*, 10490; c) M. Steenackers, S. Q. Lud, M. Niedermeier, P. Bruno, D. M. Gruen, P. Feulner, M. Stutzmann, J. A. Garrido, R. Jordan, *J. Am. Chem. Soc.* **2007**, *129*, 15655; d) M. Steenackers, I. D. Sharp, K. Larsson, N. A. Hutter, M. Stutzmann, R. Jordan, *Chem. Mater.* **2010**, *22*, 272; e) P. Xiao, J. Gu, J. Chen, D. Han, J. Zhang, H. Cao, R. Xing, Y. Han, W. Wang, T. Chen, *Chem. Commun.* **2013**, *49*, 11167; f) P. Xiao, J. Gu, J. Chen, J. Zhang, R. Xing, Y. Han, J. Fu, W. Wang, T. Chen, *Chem. Commun.* **2014**, *50*, 7103.
- [17] T. B. Stachowiak, F. Svec, J. M. J. Frechet, *Chem. Mater.* **2006**, *18*, 5950.
- [18] Q. Wei, F. Zhang, J. Li, B. Li, C. Zhao, *Polym. Chem.* **2010**, *1*, 1430.
- [19] R. Jordan, A. Ulman, J. F. Kang, M. H. Rafailovich, J. Sokolov, *J. Am. Chem. Soc.* **1999**, *121*, 1016.
- [20] C. Xu, S. E. Barnes, T. Wu, D. A. Fischer, D. M. DeLongchamp, J. D. Batteas, K. L. Beers, *Adv. Mater.* **2006**, *18*, 1427.
- [21] a) *Ellipsometry of Functional Organic Surfaces and Films*, Springer Series in Surface Sciences, (Eds: K. Hinrichs, K. J. Eichhorn), Vol. 52, Springer, Berlin/Heidelberg, Germany **2014**; b) K. Hinrichs, M. Levichkova, D. Wynands, K. Walzer, K. J. Eichhorn, P. Bäuerle, K. Leo, M. Riede, *Thin Solid Films* **2012**, *525*, 97; c) L. Ionov, A. Sidorenko, K.-J. Eichhorn, M. Stamm, S. Minko, K. Hinrichs, *Langmuir* **2005**, *21*, 8711; d) B. Pollard, E. A. Muller, K. Hinrichs, M. B. Raschke, *Nat. Commun.* **2014**, *5*.
- [22] D. Han, P. Xiao, J. Gu, J. Chen, Z. Cai, J. Zhang, W. Wang, T. Chen, *RSC Adv.* **2014**, *4*, 22759.
- [23] a) M. E. Welch, C. K. Ober, *J. Polym. Sci., Part B: Polym. Phys.* **2013**, *51*, 1457; b) M. E. Welch, C. K. Ober, *ACS Macro Lett.* **2013**, *2*, 241; c) M. A. Chavis, N. H. You, R. Maeda, M. E. Welch, C. Ohm, C. K. Ober, *Abstr. Pap. Am. Chem. S* **2012**, *53*, 283; d) M. Kim, S. Schmitt, J. Choi, J. Krutty, P. Gopalan, *Polymers* **2015**, *7*, 1346; e) A. Turchanin, A. Golzhauser, *Prog. Surf. Sci.* **2012**, *87*, 108.
- [24] a) T. Chen, I. Amin, R. Jordan, *Chem. Soc. Rev.* **2012**, *41*, 3280; b) M. Schneider, C. Fetsch, I. Amin, R. Jordan, R. Luxenhofer, *Langmuir* **2013**, *29*, 6983; c) M. Schneider, Z. Tang, M. Richter, C. Marschelke, P. Förster, E. Wegener, I. Amin, H. Zimmermann, D. Scharnweber, H. Braun, R. Luxenhofer, R. Jordan, *Macromol. Biosci.* **2015**, DOI: 10.1002/mabi.201500314.
- [25] L. C. Baxter, V. Frauchiger, M. Textor, I. ap Gwynn, R. G. Richard, *Eur. Cells Mater.* **2002**, *4*, 1.
- [26] K. Yamamoto, M. Yamamoto, H. Ooka, *Mech. Ageing Dev.* **1988**, *42*, 183.
- [27] W. M. Becker, L. J. Kleinsmith, J. Hardin, *The World of the Cell*, Benjamin-Cummings Pub. Co., San Francisco, CA, USA, **2003**.
- [28] K. Takahashi, S. Yamanaka, *Cell* **2006**, *126*, 663.
- [29] a) D. E. Discher, P. Janmey, Y. L. Wang, *Science* **2005**, *310*, 1139; b) B. Trappmann, J. E. Gautrot, J. T. Connelly, D. G. T. Strange, Y. Li, M. L. Oyen, M. A. C. Stuart, H. Boehm, B. J. Li, V. Vogel, J. P. Spatz, F. M. Watt, W. T. S. Huck, *Nat. Mater.* **2012**, *11*, 742.